Euro-Mediterranean Journal for Environmental Integration (2020) 5:63
https://doi.org/10.1007/s41207-020-00201-y

ORIGINAL PAPER

Low-cost biomass for the treatment of landfill leachate from Fez City: application of a combined coagulation–adsorption process

Imane El Mrabet[1] · Mostafa Nawdali[2] · Salah Rafqah[3] · Héctor Valdés[4] · Mourad Benzina[5] · Hicham Zaitan[1]

Received: 11 March 2020 / Accepted: 25 August 2020 / Published online: 15 October 2020

Abstract

In this work, the efficiency of a novel treatment of solid-waste landfill leachate based on coagulation and then adsorption onto a natural bioadsorbent was examined. The reduction in the chemical oxygen demand (COD), biological oxygen demand (BOD_5), turbidity, and color of the leachate from the urban sanitary landfill in Fez City (Morocco) following treatment was evaluated. Ferric chloride was used as the coagulant in the coagulation–flocculation pretreatment of the leachate, and *Cupressus sempervirens* cones were employed to adsorb the contaminants in the coagulated leachate. The optimum dose of ferric chloride was found to be 20 g per liter. The resulting coagulation process reduced the COD by 69%, the BOD_5 by 60%, and the color of the leachate by 88%. Following the adsorption of the pretreated landfill leachate on *Cupressus sempervirens* cones, the COD, BOD_5, and color of the leachate were found to be 86%, 96%, and 93% lower than their original values, respectively. The adsorption capacity of the treatment q_e was calculated as 385 mg_{O_2} g^{-1} for 1 g of *Cupressus sempervirens* cones per liter under optimal adsorption conditions (including pH 7, 25 °C, and 8 h of contact time). A study of the adsorption kinetics for the COD revealed that a pseudo-second-order model provided the best fit to the experimental kinetic data, and the equilibrium data were well described by the Langmuir isotherm model. These results of the study indicate that the novel combined coagulation–adsorption treatment of landfill leachate is an inexpensive alternative to current landfill leachate treatments, and is suitable for application to industrial-scale sanitary landfills.

Keywords Landfill leachate · Coagulation · Bioadsorbent · Adsorption

Communicated by Moncef Khadraoui, Associate Editor.

✉ Imane El Mrabet
imane.elmrabet@usmba.ac.ma

✉ Hicham Zaitan
hicham.zaitan@usmba.ac.ma

Mostafa Nawdali
mostafa.nawdali@usmba.ac.ma

Salah Rafqah
rafqah@gmail.com

Héctor Valdés
hvaldes@ucsc.cl

Mourad Benzina
mourad.benzina@enis.rnu.tn

[1] Processes, Materials and Environment Laboratory (LPME), Faculty of Sciences and Technology, Sidi Mohamed Ben Abdellah University, B.P. 2202, Fez, Morocco

[2] Processes, Materials and Environment Laboratory (LPME), Polydisciplinary Faculty, Sidi Mohamed Ben Abdellah University, B.P. 1223, Taza, Morocco

[3] Laboratoire de Chimie Analytique et Moléculaire (LCAM), Faculté Polydisciplinaire de Safi, Université Cadi Ayyad, Safi, Morocco

[4] Clean Technologies Laboratory, Universidad Católica de la Santísima Concepción, Alonso de Ribera 2850, Concepción, Chile

[5] Laboratory Water, Energy and Environment (LR3E), National Engineering School of Sfax, University of Sfax, Sfax, Tunisia

Introduction

Landfill leachate is characterized by high concentrations of organic and inorganic compounds and toxic substances (Alibardi and Cossu 2018; Youcai 2018). It is considered a source of hazardous surface-water and groundwater contamination, since it can percolate through the soil, thus degrading the environment and presenting a risk to ecosystems (Joshi and Gogate 2019). To mitigate these adverse effects and ensure that landfill leachate meets liquid discharge standards, various treatment processes such as coagulation–flocculation, precipitation, advanced oxidation technologies, ion exchange, membrane filtration, adsorption, and aerobic and anaerobic treatments have been applied individually or in combination to real or simulated liquid effluents.

It has been reported that coagulation can remove 60–67% of the COD from stabilized leachate originating from the Mohammedia landfill in Morocco. Additionally, Assou et al. (2016) noted that treatment with $FeCl_3$ and $Al_2(SO_4)_3$ removed 67 and 60% of the COD, respectively, under optimal conditions (18.5 mmol Fe^{3+} L^{-1} at pH 6.5 and 5.82 mmol Al^{3+} L^{-1} at pH 5.3). A precipitation treatment investigated by Reynier et al. (2015) reduced the concentrations of Cu, pentachlorophenol (PCP), and As in landfill leachate by 39%, 84%, and 93%, respectively.

Previous studies have shown that COD removal using advanced oxidation technologies yields promising results (El Mrabet et al. 2020; Abu Amr et al. 2014; El Mrabet et al. 2018). Treatment of a stabilized leachate from Fez (Morocco) with $S_2O_8^{2-}$/Fe/UV-A removed 70% of the COD and 94% of the color (El Mrabet et al. 2020), while applying the photo-Fenton process to the same leachate achieved an 84% reduction in COD and removed > 90% of the color (El Mrabet et al. 2018).

Moreover, an ozonation treatment that required 9.42 kg_{O_3} kg_{COD}^{-1} was applied to Malaysian semi-aerobic stabilized landfill leachate, and was found to decrease the COD, NH_3–N, and color by 26.7, 7.1, and 92%, respectively (Abu Amr et al. 2014). Ion exchange using a commercial resin that removes 7643.64 mg COD g^{-1} resin has also been evaluated as a treatment for semi-aerobic stabilized landfill leachate from Malaysia (Zamri et al. 2017). When ultrafiltration membranes were included in biological treatment systems for landfill leachate in the UK, a 60% reduction in COD values was achieved, along with the removal of 61.6% and 34.3% of the chromium and nickel in the leachate, respectively (Robinson 2017). Adsorption using 3 g L^{-1} of powder activated carbon (PAC) was employed by Chaouki et al. (2017) to reduce the COD, turbidity, and color of pretreated landfill leachate from Casablanca (Morocco) by 77%, 99%, and 99.7%, respectively. The same process was also investigated to treat raw urban wastewater from Fez City (Morocco); in this method, 0.5 g L^{-1} of the activated carbon from jujube shells was found to remove 72% of the COD and 83% of the color from the leachate (Kachabi et al. 2019). An aerobic treatment of young landfill leachate (Tunisia) characterized by a relatively high biodegradability index (BOD_5/COD=0.4) was investigated by Trabelsi et al. (2011), and the total organic carbon (TOC) removal rate was found to vary between 65% and 97%, while the reduction in COD reached 92%. A study by Van Turnhout et al. (2018) indicated that 25% removal of biodegradable carbon and 27% removal of biodegradable nitrogen were possible under aerated conditions, and that reductions of 14% and 17%, respectively, could be achieved under anaerobic conditions.

The wide variety of treatment processes that have been applied to leachate can be explained by the dependence of the effectiveness of each treatment on the age and complex composition of the leachate. Consequently, it is often necessary to combine different treatment steps to increase the effectiveness of the overall treatment.

In previous studies, combined landfill leachate treatments involving coagulation–flocculation with adsorption have been shown to substantially decrease COD: a reduction of 77% was achieved using $FeCl_3$ as coagulant and PAC as an adsorbent (Chaouki et al. 2017), 86% removal was attained with coagulation–flocculation using polyferric sulfate (PFS) followed by adsorption onto PAC (Li et al. 2010), a decrease of 82% was obtained after alum coagulation–flocculation combined with adsorption onto fly ash (Gandhimathi et al. 2013), a reduction of 90% was realized after applying sequential air stripping followed by coagulation–flocculation using $FeCl_3$ and adsorption onto chitosan beads (De et al. 2019), and a decrease of 53% was achieved using $FeCl_3$ coagulation–flocculation prior to granular activated carbon (GAC) adsorption (Oloibiri et al. 2015).

In this context, the work reported in the present paper investigated the efficiency of a novel landfill leachate treatment involving sequential coagulation and then adsorption (denoted CoaAds), in which Moroccan biomass—*Cupressus sempervirens* cones (CupSem)—is used as the adsorbent to remove landfill leachate contaminants. In a recent study (Bencheqroun et al. 2019), this CupSem bioadsorbent was observed to have a high adsorption capacity for organic pollutants (methylene blue and Congo red) in aqueous solutions. The abundance and low cost of CupSem make it a strong candidate for use as a bioadsorbent to remove COD from landfill leachate.

In the present work, landfill leachate was first characterized and then pretreated with the coagulation–flocculation process using liquid $FeCl_3$ as a coagulant, optimizing the coagulant dose and the initial pH of the leachate. Then the application of the CupSem bioadsorbent to the pretreated effluent was optimized with respect to the operational

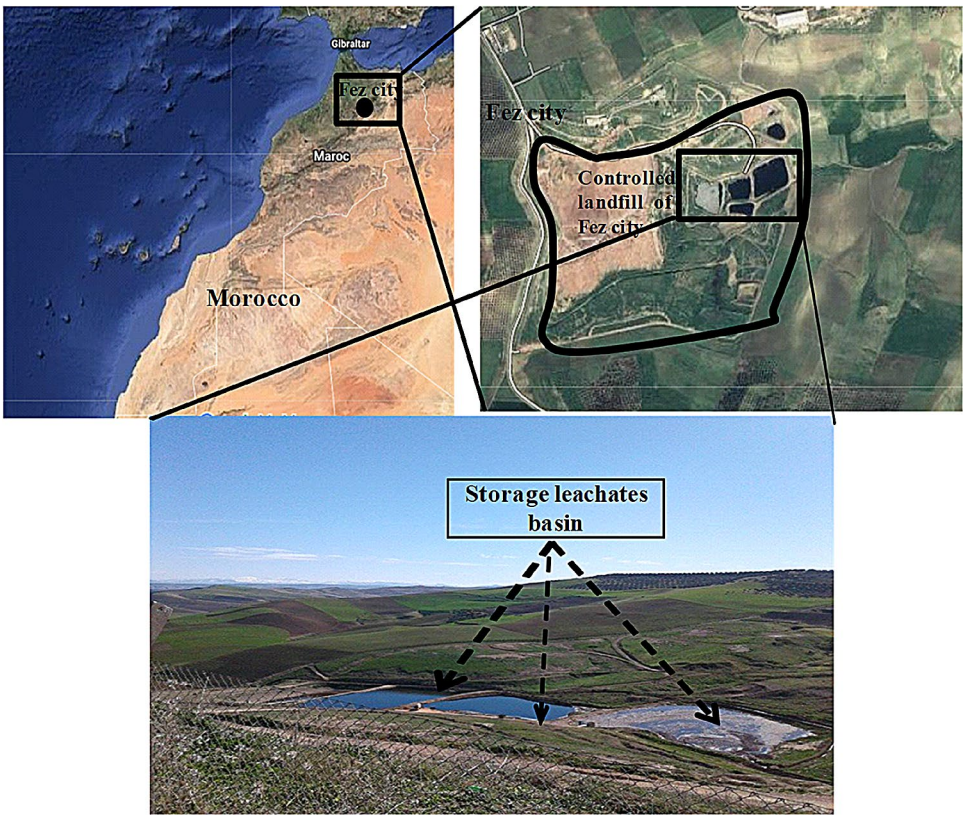

Fig. 1 Map of the location of Fez City, satellite image of the landfill in Fez, and photograph of the leachate storage basins at the landfill site

conditions (i.e., adsorbent mass, initial pH of the solution, contact time, and temperature). Treatment performance was evaluated in terms of the percentage reductions in COD, BOD_5, turbidity, sludge volume, and color.

Materials and methods

Leachate sampling

Landfill leachate samples were collected from the urban sanitary landfill of Fez City, northwestern Morocco (34°00′16.6″N, 4°55′44.5″W) (Fig. 1). The collected leachate sample was stored in opaque 25 L plastic bottles at 4 °C in order to minimize leachate decomposition caused by microbial activity.

Chemicals and materials

The coagulant—ferric chloride ($FeCl_3$), 40% w/w—was supplied in a liquid state by Cadilhac (Casablanca, Morocco).

HCl and NaOH were purchased from Sigma–Aldrich (St. Louis, MO, USA). Natural cypress cone chips from *Cupressus sempervirens* were collected from the Fez area (Morocco). The material was washed with tap water several times, and then with distilled water. After washing, it was dried at 110 °C in an oven for 24 h to eliminate volatile impurities, cut into small portions, and then crushed into 100 µm particles using a domestic mixer. The resulting powder was stored in hermetic glass bottles for future use.

Characterization of CupSem and leachate

The surface composition of the CupSem before and after the adsorption of leachate was analyzed by Fourier-transform infrared spectroscopy (FTIR) using a VERTEX70 spectrometer, which covered the range 4000–400 cm^{-1} with a resolution of 4 cm^{-1}. Basic and acid surface sites were determined via the classical Boehm titration method (Boehm 1994). The pH of the point of zero charge (pH_{pzc}) was determined using the solid addition method (Noh and Schwarz 1989). Briefly, various solutions of NaCl (50 mL, 0.1 M) with pH values between 2 and 12 were produced, after which 0.1 g of CCS were added to each NaCl solution under nitrogen bubbling. The mixtures were then stirred for 72 h at 25 °C and the final pH was measured. The pH_{pzc} was determined graphically as the point where $pH_{final} = pH_{initial}$.

X-ray diffraction (XRD) was performed using an X'Pert PRO diffractometer ($2\theta = 0–90°$; 40 kV; 30 mA; CuKα) to study the structural properties of the bioadsorbent. The morphological surface of the CupSem was analyzed using scanning electron microscopy (Quanta 200, Thermo Fisher

Scientific) coupled with energy-dispersive X-ray spectroscopy (SEM–EDX).

Leachate samples were characterized before and after each treatment. The temperature, pH, turbidity, COD, BOD_5, UV absorbance, chloride, nitrate, nitrite, and sulfate were measured according to the standard methods for the examination of water and wastewater (Bridgewater et al. 2012). UV–visible absorption measurements were obtained using a spectrophotometer (VWR UV-6300PC) equipped with quartz cuvettes with a light path length of 1 cm. Metal concentrations were determined using inductively coupled plasma atomic emission spectroscopy analysis (ICP-AES; Activa, Jobin Yvon). All leachate parameter values presented here are the averages of three replicates, and some measurements necessitated dilution.

Coagulation process

The coagulation of landfill leachate using ferric chloride was carried out using 1 L beakers in a jar-test apparatus (FP4 portable flocculator, VELP Scientifica) at room temperature. Iron(III) chloride ($FeCl_3$) was tested as a coagulant at various dosages to determine the optimal dosage and pH value that maximized the removal of turbidity, COD, and color from the leachate. Varying volumes of $FeCl_3$ (2–10 mL) were added directly to 250 mL of leachate, yielding samples containing $FeCl_3$ dosages ranging from 5 to 22 g L^{-1}. The mixture was stirred for a period of 10 min at 200 rpm and then at 40 rpm for 30 min. After that, the sludge was left to settle for 60 min in order to achieve a stable volume. Subsequently, the supernatant was collected for physicochemical measurements and for adsorption tests.

Adsorption experiments

Batch adsorption experiments were carried out to evaluate the efficiency of the bioadsorbent and to optimize the main experimental parameters: bioadsorbent dosage, pH of the solution, contact time, and temperature. The effect of bioadsorbent dosage on the COD adsorption capacity was determined by adding various amounts of bioadsorbent (0.5–14 g L^{-1}) to flasks containing 20 mL of the pretreated leachate with a fixed COD of 1400 mg O_2 L^{-1} at 25 °C.

The adsorption kinetics were examined by adding the optimal dose of CupSem to 500 mL of the pretreated leachate sample at the optimal pH. Samples were taken after various contact times ranging from 5 to 2900 min.

The effect of temperature on COD adsorption was also investigated in the range between 25 and 35 °C. At the end of each experiment, the samples were centrifuged at 4000 rpm for 10 min and the residual COD in the supernatant was analyzed. All of the parameters were fixed at their optimized values in order to maximize COD removal. The total amount of COD per unit mass of CupSem at equilibrium (q_e, mg g^{-1}), the amount of COD adsorbed at contact time t (q_t, mg g^{-1}), and the COD removal efficiency (COD removal, %) were determined, respectively, as follows:

$$q_{t,e} = \frac{(C_0 - C_{t,e})V}{m} \quad (1)$$

$$\text{COD removal} = \frac{(C_0 - C_t) \times 100}{C_0}, \quad (2)$$

where C_0 (mg/L) and $C_{t,e}$ (mg L^{-1}) are the COD concentrations at $t = 0$ and at time t or equilibrium, respectively, V is the volume of the solution (L), and m is the weight of bioadsorbent (g).

Results and discussion

Landfill leachate characterization

Table 1 summarizes the main parameters of the raw leachate from the Fez landfill. According to the Moroccan standards for liquid discharges MLDS), this leachate is characterized by very high levels of COD (6730 mg L^{-1}), BOD_5 (600 mg L^{-1}), TSS (19,128 mg L^{-1}), and turbidity

Table 1 Comparison of the physicochemical characteristics of raw landfill leachate from the Fez City landfill with the 2018 Moroccan liquid discharge standards (MLDS)

Parameter	Unit	Value (average)	MLDS
T	°C	24	30
pH	–	8	5.5–9.5
Conductivity	mS cm^{-1}	29	2700
Turbidity	NTU	248	–
TSS	mg L^{-1}	19,128	100
CN	Abs.	11.53	–
COD	mg O_2 L^{-1}	6730	500
BOD_5	mg O_2 L^{-1}	600	100
BOD_5/COD	–	0.089	–
Nitrate N	mg L^{-1}	6.58	–
Nitrite N	mg L^{-1}	6.34	–
Chloride	mg L^{-1}	7100	3010
Sulfate	mg L^{-1}	140	600
Cr	mg L^{-1}	1.736	2
Cu	mg L^{-1}	0.049	2
Fe	mg L^{-1}	1.825	5
Mn	mg L^{-1}	0.043	2
Zn	mg L^{-1}	0.200	5
Ni	mg L^{-1}	< 0.01	5

(248 NTU). The high values of these parameters may be related to the blackish color (a high color number: 11.53) of the leachate. The high COD and color number of the leachate indicate that it is highly loaded with various organic compounds (phenolic compounds, fulvic acids, aromatic hydrocarbons, carboxylic acids, and carbohydrates) (Liu et al. 2015). Another relevant characteristic is the high conductivity (29,100 µS cm^{-1}) of the leachate, which indicates that there is a large amount of dissolved inorganic material in the leachate. This inference is supported by the measured concentrations of the following ions in the leachate: Cl^- (7100 mg L^{-1}), SO_4^{2-} (140 mg L^{-1}), NO_3^- (6.58 mg L^{-1}), and NO_2^- (6.34 mg L^{-1}).

Its pH of 8 and its BOD_5/COD ratio of 0.089 (< 0.1) indicate that the landfill leachate sample is stable and that its organic matter content has low biodegradability (Baiju et al. 2018), implying that the leachate can be treated using physicochemical processes (Sruthi et al. 2018; Li et al. 2010). Heavy metals such as Cr, Cu, Fe, Mn, and Zn were also detected at concentrations of 1.736, 0.049, 1.825, 0.043, and 0.200 mg L^{-1}, respectively.

Characterization of CupSem

The spectrum of CupSem presented in Fig. 2 shows a broad and strong superimposed absorption band in the 3000–3500 cm^{-1} region, with the maximum of the band occurring at about 3350 cm^{-1}. This band may be due to overlapping bands from O–H groups in water, alcohols, phenols, or carboxylic acids and from stretching vibrations in N–H groups in aliphatic amines (Filote et al. 2016; Bulgariu and Bulgariu 2018).

Another band at 2974 cm^{-1} can be attributed to aliphatic C–H stretching in methyl and methylene groups in side chains (Haris and Sathasivam 2009). The spectrum also displays an absorption peak at 1739 cm^{-1} that corresponds to stretching vibrations of carboxyl groups (Heraldy et al. 2018; Filote et al. 2016). A peak at 1560 cm^{-1} can be assigned to conjugated hydrogen-bonded carbonyl groups, and a peak at 1454 cm^{-1} to the bending vibrations of O–H and C–H in carboxyl groups (Deniz and Aysun 2017). A band at 1040 cm^{-1} appears to be due to O–H bonds and C–OH stretching in phenolic groups (Farnane et al. 2017), –C–S in the ether groups in cellulose (Omorogie et al. 2016), or C–O–C stretching (Deniz and Aysun 2017).

Table 2 presents the chemical groups on CupSem, as identified by Boehm titration. It is noticeable that acidic (phenolic, lactonic, and carboxylic) groups are more abundant than basic groups. These results suggest that CupSem is acidic, which is consistent with its FTIR spectrum and the previously measured pH_{PZC} value (6.0).

X-ray diffraction (XRD) analysis was used to explore the crystallographic behavior of CupSem. The resulting diffraction patterns are illustrated in Fig. 3. The pattern exhibits a feature arising from the amorphous phase (carbonaceous material) of the bioadsorbent. This is in accord with the results obtained from elemental analysis (EDX; Fig. 4c), which indicated that CupSem has a high carbon percentage (42.75%). The XRD spectrum also shows two characteristic peaks from the (110) and (200) diffraction planes of crystalline cellulose at 2θ = 14.78° and 22.43°, respectively (Wu et al. 2014; Casas

Table 2 Chemical groups on the surface of CupSem

Functional groups	Carboxylic function	Lactonic function	Phenolic function	Acid function	Basic function
Value (meq L^{-1})	0.1	1.03	0.39	1.52	0.87

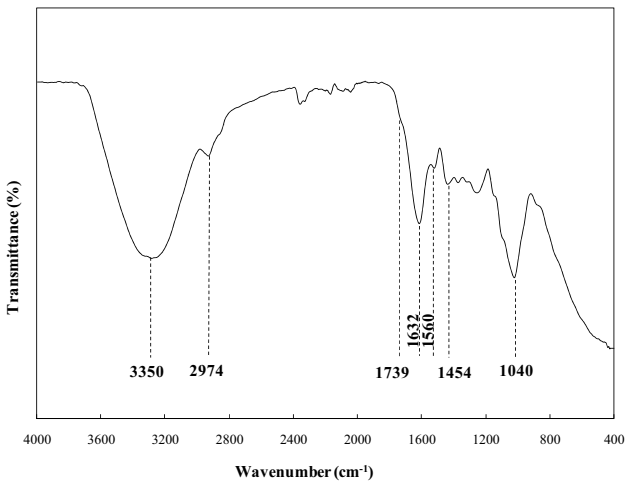

Fig. 2 FTIR spectrum of CupSem

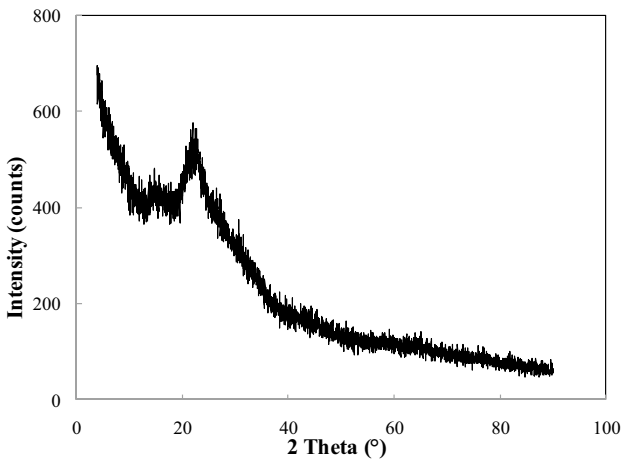

Fig. 3 XRD pattern of CupSem

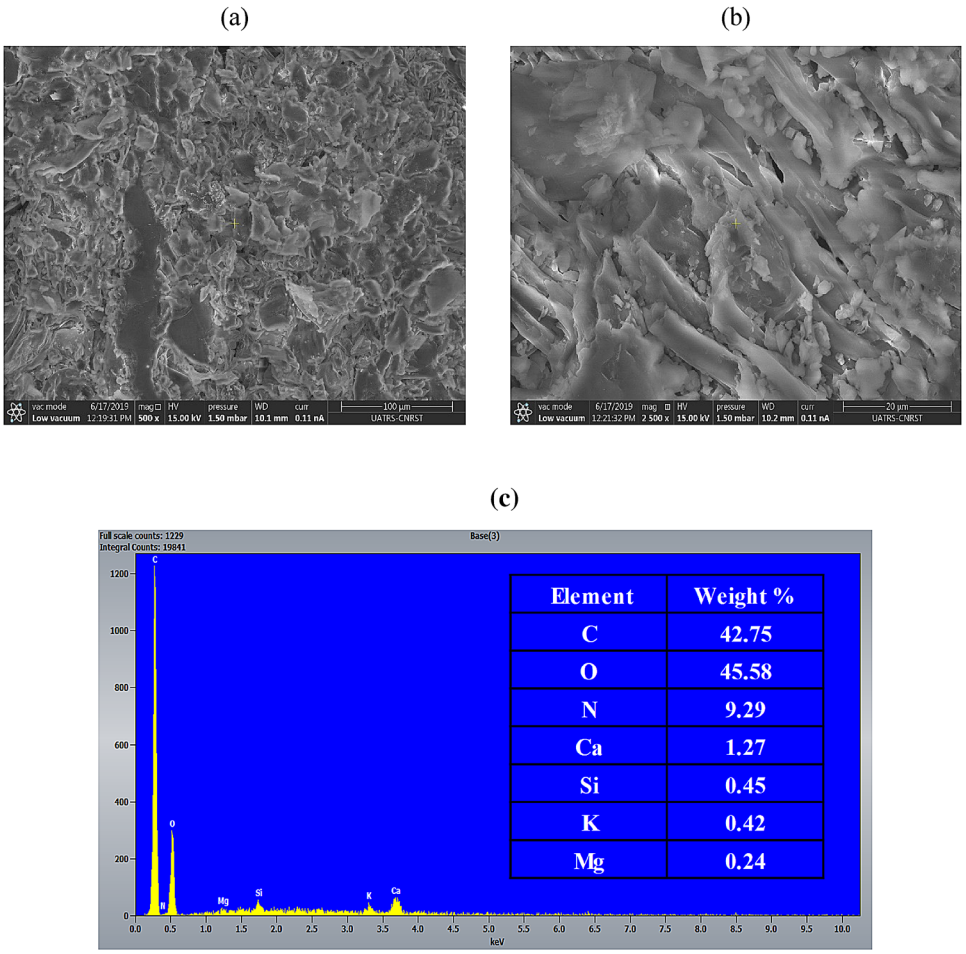

Fig. 4 Scanning electron microscopy images of CupSem (**a** ×500 and **b** ×2500) and the corresponding EDX spectrum (**c**)

et al. 2013). The presence of cellulose should enhance the adsorptive properties of CupSem, given that many studies have used cellulose-based adsorbents to remove various contaminants from aqueous solutions (Kumar et al. 2017; Maaloul et al. 2017; Liu et al. 2018a).

The surface morphology of CupSem was observed by scanning electron microscopy, as shown in Fig. 4a, b. Particles of the CupSem bioadsorbent were noted to have irregular forms and different sizes, and a well-developed surface morphology was clearly visible along with the presence of a heterogeneous porous structure.

The EDX spectrum of CupSem (Fig. 4c) confirms that carbon and oxygen are the main elements that constitute this biomass, as they produce the most intense peaks and have the highest weight percentages.

Coagulation–flocculation process

Effect of coagulant dosage

Figure 5 shows how the UV–visible spectrum of the leachate in the wavelength range 200–700 nm varied with the $FeCl_3$ dosage applied. As illustrated in Fig. 5, increasing the $FeCl_3$ dosage clearly reduced the absorbance, especially in the wavelength range 200–300 nm, which initially (i.e., before treatment) contained peaks due to polycyclic aromatic compounds and macromolecular organic matter with carbonyl

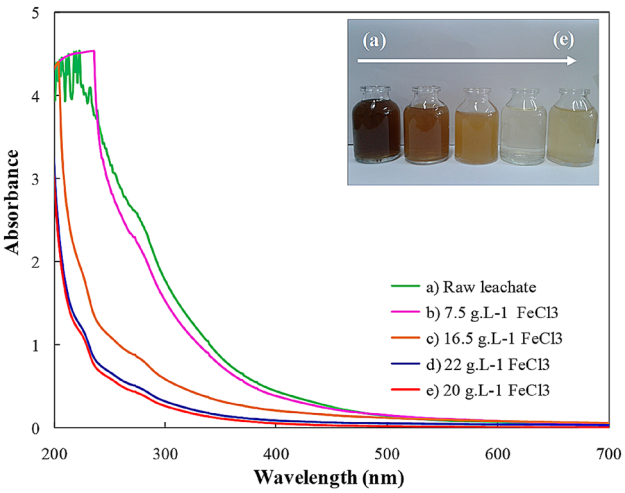

Fig. 5 Effects of $FeCl_3$ dosage on the UV–visible spectrum and color of the landfill leachate

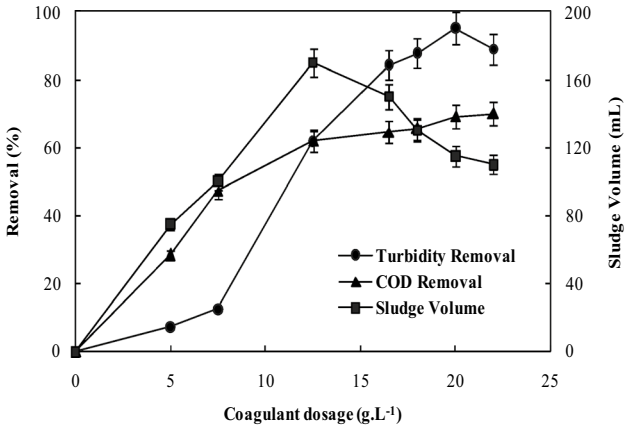

Fig. 6 Influence of the ferric chloride dosage on the turbidity and COD removal efficiencies and the resulting sludge volume

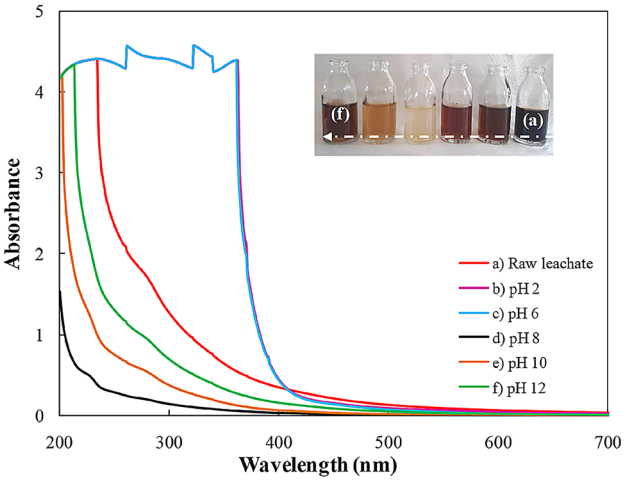

Fig. 7 Effect of initial leachate pH on the UV–visible spectrum and color of leachate treated with a $FeCl_3$ dosage of 20 g L^{-1}

groups and conjugated double bonds (Liu et al. 2018b; Luo et al. 2018). This decline in the absorbance with $FeCl_3$ dosage correlates with the visual aspects of these samples shown in the photograph in Fig. 5, where the intensity of the color of the leachate decreases as the coagulant dosage increases (dark brown → clear yellow). The weakest color intensity was observed for the sample treated with 20 g L^{-1} of $FeCl_3$. These results indicate that some of the aromatic compounds in the leachate were removed by the coagulation process when using $FeCl_3$ as a coagulant.

To further investigate the effect of the ferric chloride coagulant, its dose was varied from 5 to 22 g L^{-1}, and measurements of COD, turbidity, and sludge volume were performed. From Fig. 6, it is apparent that increasing the $FeCl_3$ dosage enhanced the COD removal efficiency from 28 to 69% and the turbidity removal efficiency from 6 to 95%. However, when the coagulant dosage was increased from 20 g L^{-1} to 22 g L^{-1}, the change in the COD removal efficiency was insignificant (+ 1%), and the turbidity removal efficiency decreased slightly to 89%. This behavior can be explained by the phenomenon of charge neutralization, where the addition of the optimal amount of Fe^{3+} neutralizes the negative charge on the suspended colloids, destabilizing them and thus enhancing the coagulation process. However, when the coagulant dosage exceeds the optimal value, the colloids restabilize due to the charge repulsion caused by the presence of excess Fe^{3+} ion (Li et al. 2010; Ishak et al. 2018).

The volume of sludge generated rose from 30 to 68% v/v (volume of sludge/volume of leachate) as the coagulant dosage was increased from 5 to 12.5 g $FeCl_3$ L^{-1}. The volume of sludge then decreased with increasing coagulant dosage until it reached 53.6% v/v for a dosage of 22 g $FeCl_3$ L^{-1}.

Overall, these results indicate that the optimum dose of ferric chloride was 20 g L^{-1}, as this dosage led to reductions in turbidity and COD of 95% and 69%, respectively.

A significant decrease in pH from 7.6 to 5.9 was observed upon increasing the $FeCl_3$ dosage from 5 to 22 g L^{-1}. This drop in pH can be explained by the highly acidic nature of $FeCl_3$ (Amokrane et al. 1997; Racar et al. 2017), as well as by the decrease in alkaline compounds present in the leachate upon adding more coagulant.

Effect of initial leachate pH on coagulation–flocculation

In order to study the effect of pH on the turbidity and COD of the leachate, the initial leachate pH was adjusted to 2, 4, 6, 10, or 12 before adding 20 g L^{-1} $FeCl_3$.

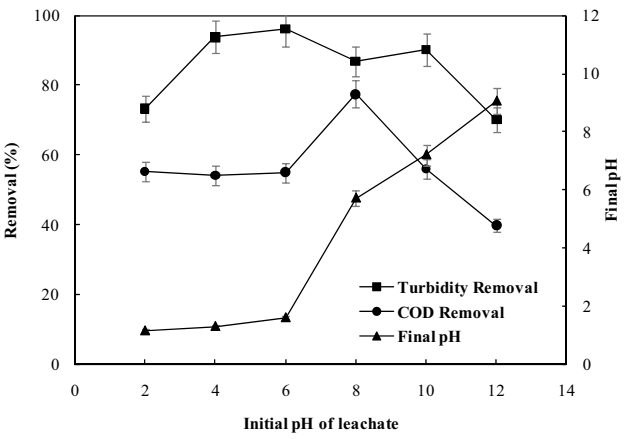

Fig. 8 Inflence of the initial pH of the raw leachate on the COD, turbidity, and pH of the leachate treated with a $FeCl_3$ dosage of 20 g L^{-1}

Figure 7 indicates the effect of the initial leachate pH on the UV–visible spectrum of the treated leachate. The results show that treated samples that initially had an acid pH (pH < 7) were characterized by high absorbance and a dark color. On the other hand, the absorbance in the wavelength range 200–400 nm was significantly lower than that of the raw leachate when the initial pH was 8, 10, or 12. In particular, the treated sample with no initial pH adjustment (i.e., pH 8) showed the lowest absorbance and the weakest color.

The results shown in Figs. 7 and 8 confirm that the optimal initial pH of the leachate is 8, which is the pH of the raw leachate without any adjustment.

Figure 8 shows the influence of the initial leachate pH on the COD, turbidity, and final pH of the treated leachate. It is worth noting that increasing the initial solution pH from 2 to 6 led to the same COD removal efficiency (almost 55%), an improvement in turbidity removal efficiency from 73 to 96%, and a final pH of ~ 1.5.

Applying an initial pH of 8 (i.e., no initial pH adjustment) led to the greatest drop in COD and turbidity (77% and 87%, respectively) and a final pH of 5.7. Increasing the leachate pH from 10 to 12 reduced the COD removal efficiency from 56% to 40% and the turbidity removal efficiency from 90% to 70%.

It is known that the $FeCl_3$ is generally most efficient as a coagulant in the pH range between 4 and 5. Under acidic conditions, ferric ions can hydrolyze and form polynuclear cations with multiple positive charges, such as $Fe(OH)^{2+}$, $Fe_2(OH)_2^{4+}$, $Fe_3(OH)_4^{5+}$, and/or other such cations (Li et al. 2010). Meanwhile, under basic conditions, the reaction between Fe^{3+} and OH^- can result in the formation of $Fe(OH)_3$, $Fe(OH)_4^-$, and $Fe(OH)^-$. Consequently, due to the negative charge on the colloids, polynuclear cations are more preferable than the species formed under basic conditions (Ishak et al. 2018), thus explaining the low COD removal at high pH values (10 and 12). However, it was reported by Gandhimathi et al. (2013) that the $Fe(OH)_3$ precipitate can trap pollutants, which explains the relatively high COD elimination efficiencies (56% and 40%) obtained at high pH values (10 and 12, respectively).

Although the optimal pH range of $FeCl_3$ is said to be 4–5, the coagulant was most efficient at a higher pH (8) in our study. This result can be explained by the fact that the colloids in the landfill leachate are negatively charged and are stable in the pH range of 5–9 (Ishak et al. 2018); high availability of negative colloids would consequently enhance the formation of macromolecular complexes between the colloids and $FeCl_3$ (Kurup et al. 2019).

In addition, several studies have investigated the optimal pH to remove the maximum amount of organic matter during the coagulation–flocculation process. The optimal pH values elucidated in those studies varied considerably: 5.2 was the optimal pH to eliminate 55.3% of the COD with 3.1 g L^{-1} of $FeCl_3$ (De et al. 2019), pH 6 and a COD:$FeCl_3$ ratio of 1:1.3 removed 70% of the COD (Ishak et al. 2018), pH 7.9 and 1.4 g L^{-1} of $FeCl_3$ reduced COD by 66% (Oloibiri et al. 2015), pH 10 and 3 g L^{-1} of $FeCl_3$ yielded a COD removal efficiency of 70% (Kumar and Bishnoi 2017), and 53.8% of the dissolved organic carbon was removed with 280 mg L^{-1} Fe(III) at pH 3 (Chu et al. 2020). This significant variation in the optimal pH could be due to the large variety of compounds in the leachate that influence the charge on the suspended solids in the leachate (Zazouli and Yousefi 2008).

In order to prepare the pretreated leachate for the adsorption tests, the initial pH was fixed at the optimal pH (8, the pH of raw leachate), and the optimal coagulant dose of 20 g $FeCl_3$ L^{-1} was applied in the raw leachate pretreatment.

Adsorption process

Effect of the bioadsorbent dosage

Experiments were carried out in which bioadsorbent dosages in the range 0.5–14 g L^{-1} were applied to leachate samples with an initial concentration of organic matter (COD) of 1400 mg O_2 L^{-1} at pH 6.86 and 25 °C until equilibrium was attained. All experiments were carried out in duplicate.

The effect of the bioadsorbent dosage on the COD adsorption capacity was examined by introducing 20 mL of the leachate sample pretreated with ferric chloride and with a fixed COD of 1400 mg O_2 L^{-1} into flasks and adding various amounts of the bioadsorbent (0.5–14 g L^{-1}) to the flasks at 25 °C.

The effects of varying the CupSem dosage on COD removal and COD adsorption are depicted in Fig. 9.

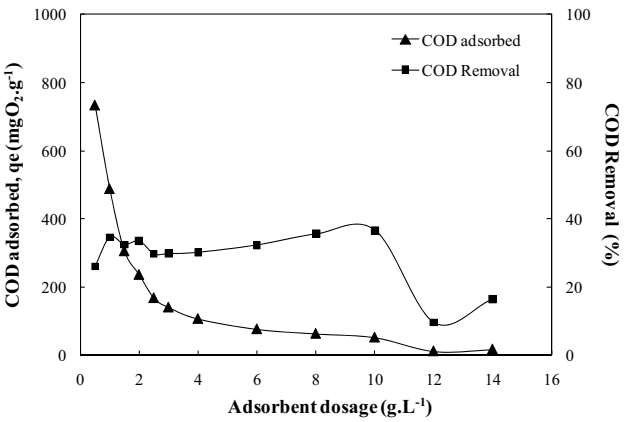

Fig. 9 Effects of the CupSem dosage on COD removal and COD adsorption (initial COD = 1400 mg L^{-1}, T = 25 °C, pH 6.86)

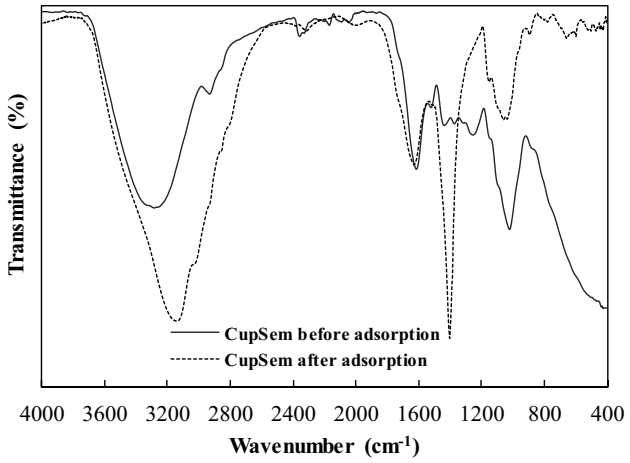

Fig. 10 FTIR spectra of CupSem before and after adsorption

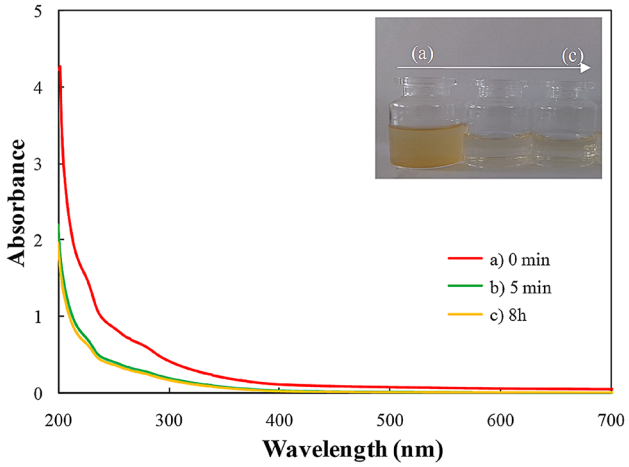

Fig. 11 UV–visible spectrum and leachate color before and during treatment involving adsorption onto CupSem: **a** 0 min, **b** 5 min, and **c** 8 h of adsorption time

As seen from Fig. 9, increasing the bioadsorbent dosage from 0.5 to 1 g L^{-1} leads to the greatest reduction in COD (35%), which is due to the high availability of adsorption sites. Increasing the bioadsorbent dosage beyond this level caused the COD removal efficiency to decrease slightly before stabilizing until the dose is increased to 10 g L^{-1}. Above this value, the COD removal efficiency drops off, probably due to bioadsorbent particle aggregation and overcrowding, which would hinder the approach of molecules to adsorption sites on the CupSem, thus lowering the amount of pollutants adsorbed per unit of bioadsorbent. Therefore, 1 g L^{-1} was considered to be the optimal dosage of bioadsorbent to be applied in subsequent tests.

The CupSem–leachate interaction was studied by performing a FTIR analysis of CupSem before and after adsorption. These FTIR spectra are presented in Fig. 10.

Comparison of the FTIR spectra of CupSem before and after adsorption in the range of 400–4000 cm^{-1} allowed us to identify the functional groups that are responsible for the removal of organic matter from the leachate. The two FTIR spectra clearly present the same functional groups, but the spectra differ in the intensities of their peaks. This can be explained by the formation of a matrix with a crosslinked network between CupSem and the organic matter in the leachate.

Adsorption kinetics

The kinetics of the adsorption process were investigated in order to determine the contact time required to reach equilibrium and to elucidate the adsorption mechanism. Experiments were conducted using a constant volume of leachate (500 mL). The initial concentration of organic matter was expressed as the COD (400 mg O_2 L^{-1}). The mass of CupSem per liter of aqueous solution was 1 g L^{-1}.

Figure 11 presents the UV–visible spectrum of the leachate as a function of contact time. The absorbance of the leachate was observed to have decreased substantially after only 5 min of adsorption onto the CupSem bioadsorbent and to have decreased slightly more after 8 h of adsorption, which explains the lack of color of the solutions obtained after 5 min and 8 h, as shown in the photograph in Fig. 11.

Figure 12 presents the variation in the amount of COD adsorbed onto the CupSem bioadsorbent versus contact time when a bioadsorbent dosage of 1 g per liter of leachate was applied. It is clear from Fig. 12 that the adsorption process initially proceeded rapidly due to the high availability of free adsorption sites at the start of treatment (Li et al. 2010; Foo et al. 2013). As the system neared equilibrium, the process

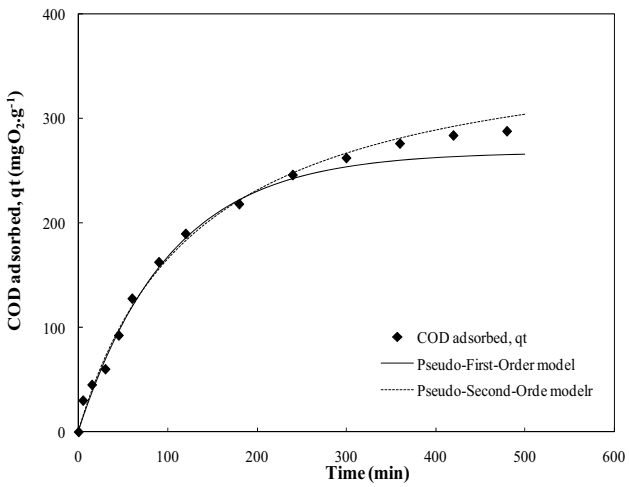

Fig. 12 Effect of contact time on the efficiency of pretreated leachate adsorption onto CupSem (initial COD = 705 mg L^{-1}, m = 1 g L^{-1}, T = 25 °C, pH 6.86)

gradually slowed. This phenomenon can be attributed to a reduction in instant solute adsorption due to a lack of available sites for COD uptake, which in turn suggests that the adsorption occurred via film diffusion (Fujiki et al. 2011). The time required to adsorb the majority of the COD and reach equilibrium was 24 h. The COD uptake profile is a single smooth and continuous curve until saturation, which suggests that a COD monolayer is formed on the CupSem surface.

In order to examine the behavior of the CupSem bioadsorbent and to identify the dominant adsorption mechanism, pseudo-first-order and pseudo-second-order models were applied to the experimental data. The models were analyzed based on the regression coefficient (R^2) and the amount of COD adsorbed at equilibrium. The pseudo-first-order kinetic model (Lagergren 1889) is

$$q_t = q_e(1 - e^{-k_1 t}), \tag{3}$$

where q_t and q_e (mg g^{-1}) are the adsorption capacities at time t and equilibrium, respectively, and k_1 (min^{-1}) is the rate constant of the pseudo-first-order model, which can be obtained by plotting q_t versus t.

The pseudo-second-order kinetic model reported by Ho and Mckay (Ho and Mckay 1999) is

$$q_t = \frac{k_2 q_e^2 t}{1 + k_2 q_e t}, \tag{4}$$

where k_2 (g mg^{-1} min^{-1}) is the adsorption rate constant.

The parameters of the two kinetic models after they had been fitted to the experimental data are listed in Table 3. The regression coefficients (R^2) for the models indicate that the experimental data are fitted better by the pseudo-second-order model ($R^2 = 0.97$) than by the pseudo-first-order model ($R^2 = 0.93$), which in turn indicates that the adsorption of COD on CupSem is mainly mediated by chemical interactions—the formation of covalent bonds through the exchange of electrons between the studied bioadsorbent and the leachate compounds (Wang et al. 2019; Zarghami et al. 2016).

Table 3 Kinetic parameters for the adsorption of COD onto CupSem

Kinetic model	Parameter	Value
Pseudo-first-order model	q_e (mg g^{-1})	268
	K_1	0.0098
	R^2	0.93
Pseudo-second-order model	q_e (mg g^{-1})	385
	K_2	1.95×10^{-5}
	R^2	0.97

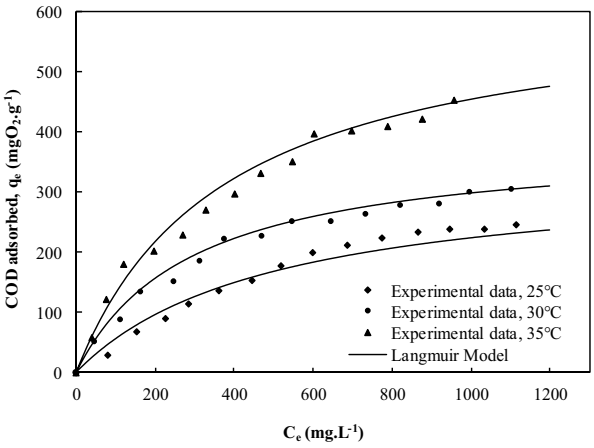

Fig. 13 Equilibrium data on the adsorption of the pretreated leachate onto the CupSem bioadsorbent (initial COD = 1400 mg L^{-1}, contact time = 24 h, m = 1 g L^{-1}, pH 6.86)

Adsorption isotherms

Adsorption models are fitted to experimental adsorption data in order to identify the interactions between the adsorbate and adsorbent surface, which can then be used to optimize the adsorption process (Hameed and Ahmad 2009; Wang et al. 2019). Thus, experimental data on the adsorption of COD onto CupSem at three different temperatures (25, 30, and 35 °C) (Fig. 13) were fitted to the Langmuir isotherm model (Langmuir 1916) in this work.

Adsorption isotherm models express the quantity of COD adsorbed per mass of CupSem, q_e (mg g^{-1}), as a function of the equilibrium COD concentration, C_e (mgO_2 L^{-1}), using the Langmuir equation,

$$q_e = \frac{q_m K_L C_e}{1 + K_L C_e}. \tag{5}$$

Here, q_m (mg O_2 g^{-1}) is the maximum adsorption capacity of the bioadsorbent, which is related to the monolayer adsorption capacity, and K_L (L mg^{-1}) is the equilibrium Langmuir adsorption constant, which is related to the affinity of the adsorbed species for the binding site.

Table 4 Isotherm parameters and correlation coefficients calculated for the adsorption of pretreated leachate onto CupSem bioadsorbent

	Parameter	T = 25 °C	T = 30 °C	T = 35 °C
Langmuir	q_m (mg g^{-1})	335	384	460
	K_L (L g^{-1})	0.000385	0.0034	0.0027
	R^2	0.98	0.99	0.98

Table 5 Comparison of adsorption capacity values of different adsorbents

Adsorbent	Adsorbate	Effluent	Adsorption capacity (mg g^{-1})	Reference
CupSem	COD	Landfill leachate pretreated with coagulation–flocculation	385	Present study
Periwinkle shell-based granular activated carbon	COD	Industrial wastewater	29.55	Badmus and Audu (2009)
Granular activated carbon from tamarind fruit seed	COD	Semi-aerobic landfill leachate	64.93	Foo et al. (2013)
Commercial powder activated carbon	COD	Landfill leachate pretreated with coagulation–flocculation	182	Chaouki et al. (2017)
Prepared activated carbon from jujube shells	COD	Raw urban wastewater	1000	Kachabi et al. (2019)
Zeolite	COD	Semi-aerobic landfill leachate	2.35	Halim et al. (2010)
Biosorbent	Lead ions	Wastewater	113.84	Wen et al. (2018)
Commercial granular activated carbon	COD	Biologically pretreated leachate	62.2	Mohammad-Pajooh et al. (2018)

The amount of COD adsorbed at equilibrium (q_e) as a function of the equilibrium COD concentration (C_e) is presented in Fig. 13, and the isotherm parameters are listed in Table 4. The calculated regression coefficient $R^2 \approx 1$ for the three temperatures, indicating that the experimental data for the adsorption of COD onto CupSem are well fitted and described by the Langmuir model. This suggests that a monolayer adsorption process takes place, that the adsorption sites are identical, and that the surface of the adsorbent is homogeneous (Gupta et al. 2016; Kumar et al. 2017).

The bioadsorbent used in this work showed a relatively high adsorption capacity for COD (335 mg g^{-1}) compared with the COD adsorption capacities of other adsorbents under similar conditions, as reported in the literature (Foo et al. 2013; Halim et al. 2010; Badmus and Audu 2009). Indeed, for comparison purposes, Table 5 presents the adsorption capacities of various natural and commercial adsorbents (including CupSem) that have been utilized to remove COD from effluents. It is clear that the CupSem studied in this work has a relatively high adsorption

Table 6 Combined efficiency of the CoaAds process in terms of pollutant removal from landfill leachate

Parameter	Unit	Raw leachate	Coagulation by $FeCl_3$	Combined coagulation and adsorption	Total removal (%)
T	°C	24	24	27	–
pH	–	8	6.8	7.2	–
Conductivity	mS/cm^2	23.7	35.1	25	–
Turbidity	NTU	237	12	8	97
TSS	mg L^{-1}	19,127.5	15,080	8570	55
CN	–	2.22	0.258	0.156	93
TA	mg L^{-1}	0	0	0	–
TAC	mg L^{-1}	407	230	20	95
COD	mg L^{-1}	6734	2077	923	86
BOD_5	mg L^{-1}	600	240	25	96
Nitrates	mg L^{-1}	6.58	0.172	0.89	86
Nitrites	mg L^{-1}	6.34	0.45	2.9	54
Phosphates	mg L^{-1}	0.27	0.0012	0.001	99.9
Ammonium	mg L^{-1}	710	305	138	81
Cr	mg L^{-1}	1.74	< 0.01	< 0.01	100
Cu	mg L^{-1}	0.05	0.12	< 0.01	100
Fe	mg L^{-1}	1.82	18.09	0.1321	93
Mn	mg L^{-1}	0.04	13.39	< 0.01	100

capacity compared to the other adsorbents investigated in other research works.

Treatment efficiency

Treatment of Fez landfill leachate using a combination of the two processes described above—coagulation followed by adsorption—led to the removal of 97% of the turbidity, 55% of the TSS, 93% of the CN, 95% of the TAC, 86% of the COD, 96% of the BOD_5, 86% of the nitrates, 56% of the nitrites, 99.9% of the phosphates, 81% of the ammonium, and > 93% of the heavy metals from the leachate (Table 6). These removal efficiencies indicate that the overall CoaAds process effectively removed the majority of the pollutants from the studied landfill leachate.

Conclusion

This study demonstrated the efficiency of a novel landfill leachate treatment while also valorizing a natural material as a low-cost bioadsorbent.

The efficiency of this treatment, which involved coagulation–flocculation of the leachate coupled with adsorption onto CupSem, was evaluated in terms of COD, turbidity, and color removal. The results presented in this paper demonstrate that the coagulation pretreatment process using a dosage of 20 g L^{-1} of ferric chloride at pH 8 removed almost all of the turbidity (95%) and much of the COD (69%) from the leachate. Pretreatment of the leachate with coagulation followed by adsorption onto the natural bioadsorbent CupSem resulted in the removal of 86%, 96%, and 93% of the COD, BOD_5, and color, respectively, under optimum conditions (a bioadsorbent dosage of 1 g L^{-1}, pH 7, and a contact time of 8 h). The adsorption of COD was best described by the Langmuir isotherm model, suggesting that it may proceed via monolayer adsorption of the COD onto CupSem. Our results indicate that a combined process involving coagulation using iron chloride as the coagulant followed by adsorption onto CupSem is a promising treatment for leachate from the Fez landfill.

Author contributions All authors actively contributed to this work by analyzing, discussing, interpreting, and checking the data. They all approved this version for publication.

Compliance with ethical standards

Conflict of interest The authors declare that they have no conflict of interest to disclose.

References

Abu Amr SS, Aziz HA, Bashir MJK (2014) Application of response surface methodology (RSM) for optimization of semi-aerobic landfill leachate treatment using ozone. Appl Water Sci 4:231–239. https://doi.org/10.1007/s13201-014-0156-z

Alibardi L, Cossu R (2018) Leachate generation modeling. In: Cossu R, Stegmann R (eds) Solid waste landfilling (concepts, processes, technologies). Elsevier Inc., Oxford, pp 229–245

Amokrane A, Comel C, Veron J (1997) Landfill leachates pretreatment by coagulation-flocculation. Water Res 31:2775–2782. https://doi.org/10.1016/S0043-1354(97)00147-4

Assou M, El Fels L, El Asli A, Fakidi H, Souabi S, Hafidi M (2016) Landfill leachate treatment by a coagulation-flocculation process: effect of the introduction order of the reagents. Desalin Water Treat 57:21817–21826. https://doi.org/10.1080/19443994.2015.1127779

Badmus MAO, Audu TOK (2009) Periwinkle shell: based granular activated demand (COD) in industrial wastewater. Can J Chem Eng 87:69–77. https://doi.org/10.1002/cjce.20140

Baiju A, Gandhimathi R, Ramesh ST, Nidheesh PV (2018) Combined heterogeneous electro-Fenton and biological process for the treatment of stabilized landfill leachate. J Environ Manage 210:328–337. https://doi.org/10.1016/j.jenvman.2018.01.019

Bencheqroun Z, El Mrabet I, Kachabi M, Nawdali M, Valdés H, Neves I, Zaitan H (2019) Removal of basic and acid dyes from aqueous solutions using cone powder from Moroccan Cypress *Cupressus sempervirens* as a natural adsorbent. Desalin Water Treat 166:387–398. https://doi.org/10.5004/dwt.2019.24514

Boehm HP (1994) Some aspects of the surface chemistry of carbon blacks and other carbons. Carbon N Y 32:759–769

Bridgewater L, American Public Health Association, American Water Works Association, Water Environment Federation (2012) Standard methods for the examination of water and wastewater, 22nd edn. American Public Health Association, Washington, DC

Bulgariu L, Bulgariu D (2018) Functionalized soy waste biomass—a novel environmental-friendly biosorbent for the removal of heavy metals from aqueous solution. J Clean Prod 197:875–885. https://doi.org/10.1016/j.jclepro.2018.06.261

Casas A, Alonso MV, Oliet M, Santos TM, Rodriguez F (2013) Characterization of cellulose regenerated from solutions of pine and eucalyptus woods in 1-allyl-3-methilimidazolium chloride. Carbohydr Polym 92:1946–1952. https://doi.org/10.1016/j.carbpol.2012.11.057

Chaouki Z, Khalil F, Ijjaali M, Valdés H, Rafqah S, Sarakha M, Zaitan H (2017) Use of combination of coagulation and adsorption process for the landfill leachate treatment from Casablanca City. Desalin Water Treat 83:262–271. https://doi.org/10.5004/dwt.2017.20743

Chu D, Ye Z, Chen S (2020) Interactions among low-molecular-weight organics, heavy metals, and Fe(III) during coagulation of landfill leachate nanofiltration concentrate. Waste Manag 104:51–59. https://doi.org/10.1016/j.wasman.2020.01.015

De S, Hazra T, Dutta A (2019) Treatment of landfill leachate by integrated sequence of air stripping, coagulation–flocculation and adsorption. Environ Dev Sustain 21:1–21. https://doi.org/10.1007/s10668-017-0053-3

Deniz F, Aysun R (2017) Bioremoval of malachite green from water sample by forestry waste mixture as potential biosorbent. Microchem J 132:172–178. https://doi.org/10.1016/j.microc.2017.01.015

El Mrabet I, Kachabi M, Nawdali M, Harrach A, Khalil F, Ijjaali M, Benzina M, Zaitan H (2018) Treatment of landfill leachate from Fez City (Morocco) using Fenton and photo-Fenton

processes. IOP Conf Ser Earth Environ Sci 161:1–10. https://doi.org/10.1088/1755-1315/161/1/012025

El Mrabet I, Benzina M, Zaitan H (2020) Optimization of persulfate/iron(II)/UV-A irradiation process for the treatment of landfill leachate from Fez City (Morocco). SN Appl Sci 2:1042. https://doi.org/10.1007/s42452-020-2868-z

Farnane M, Tounsadi H, Elmoubarki R, Mahjoubi FZ, Elhalil A, Saqrane S, Abdennouri M, Qourzal S, Barka N (2017) Alkaline treated carob shells as sustainable biosorbent for clean recovery of heavy metals: kinetics, equilibrium, ions interference and process optimisation. Ecol Eng 101:9–20. https://doi.org/10.1016/j.ecoleng.2017.01.012

Filote C, Ungureanu G, Boaventura R, Santos S, Volf I, Botelho C (2016) Green macroalgae from the Romanian coast of Black Sea: physico-chemical characterization and future perspectives on their use as metal anions biosorbents. Process Saf Environ Prot 108:34–43. https://doi.org/10.1016/j.psep.2016.06.002

Foo KY, Lee LK, Hameed BH (2013) Batch adsorption of semi-aerobic landfill leachate by granular activated carbon prepared by microwave heating. Chem Eng J 222:259–264. https://doi.org/10.1016/j.cej.2013.02.032

Fujiki J, Shinomiya T, Kawakita T, Ishibashi S, Furuya E (2011) Experimental determination of fluid-film mass transfer coefficient from adsorption uptake curve. Chem Eng J 173:49–54. https://doi.org/10.1016/j.cej.2011.07.035

Gandhimathi R, Durai NJ, Nidheesh PV, Ramesh ST, Kanmani S (2013) Use of combined coagulation-adsorption process as pretreatment of landfill leachate. Iran J Environ Heal Sci Eng 10:1–7. https://doi.org/10.1186/1735-2746-10-24

Gupta N, Kushwaha AK, Chattopadhyaya MC (2016) Application of potato (*Solanum tuberosum*) plant wastes for the removal of methylene blue and malachite green dye from aqueous solution. Arab J Chem 9:S707–S716. https://doi.org/10.1016/j.arabjc.2011.07.021

Halim AA, Aziz HA, Johari MAM, Ariffin KS (2010) Comparison study of ammonia and COD adsorption on zeolite, activated carbon and composite materials in landfill leachate treatment. Desalination 262:31–35. https://doi.org/10.1016/j.desal.2010.05.036

Hameed BH, Ahmad AA (2009) Batch adsorption of methylene blue from aqueous solution by garlic peel, an agricultural waste biomass. J Hazard Mater J 164:870–875. https://doi.org/10.1016/j.jhazmat.2008.08.084

Haris MRHM, Sathasivam K (2009) The removal of methyl red from aqueous solutions using banana. Am J Appl Sci 6:1690–1700

Heraldy E, Lestari WW, Permatasari D, Arimurti DD (2018) Biosorbent from tomato waste and apple juice residue for lead removal. J Environ Chem Eng 6:1201–1208. https://doi.org/10.1016/j.jece.2017.12.026

Ho YS, Mckay G (1999) Pseudo-second order model for sorption processes. Process Biochem 34:451–465

Ishak AR, Hamid FS, Mohamad S, Tay KS (2018) Stabilized landfill leachate treatment by coagulation-flocculation coupled with UV-based sulfate radical oxidation process. Waste Manag 76:575–581. https://doi.org/10.1016/j.wasman.2018.02.047

Joshi SM, Gogate PR (2019) Treatment of landfill leachate using different configurations of ultrasonic reactors combined with advanced oxidation processes. Sep Purif Technol 211:10–18. https://doi.org/10.1016/j.seppur.2018.09.060

Kachabi M, El Mrabet I, Benchekroun Z, Nawdali M, Zaitan H (2019) Synthesis and adsorption properties of activated carbon from KOH-activation of Moroccan jujube shells for the removal of COD and color from wastewater. Mediterr J Chem 8:168–178. https://doi.org/10.13171/10.13171/MJC8319050704HZ

Kumar SS, Bishnoi NR (2017) Coagulation of landfill leachate by $FeCl_3$: process optimization using Box-Behnken design (RSM). Appl Water Sci 7:1943–1953. https://doi.org/10.1007/s13201-015-0372-1

Kumar R, Sharma RK, Singh AP (2017) Cellulose based grafted biosorbents—journey from lignocellulose biomass to toxic metal ions sorption applications—a review. J Mol Liq 232:62–93. https://doi.org/10.1016/j.molliq.2017.02.050

Kurup GG, Adhikari B, Zisu B (2019) Treatment performance and recovery of organic components from high pH dairy wastewater using low-cost inorganic ferric chloride precipitant. J Water Process Eng 32:100908. https://doi.org/10.1016/j.jwpe.2019.100908

Lagergren S (1889) About the theory of so called adsorption of soluble substances. K Sven Vetenskapsakademiens 24:4–5

Langmuir I (1916) The constitution and fundamental properties of solids and liquids. Part I. Solids. J Am Chem Soc 38:2221–2295. https://doi.org/10.1021/ja02268a002

Li W, Hua T, Zhou Q, Zhang S, Li F (2010) Treatment of stabilized landfill leachate by the combined process of coagulation/flocculation and powder activated carbon adsorption. Desalination 264:56–62. https://doi.org/10.1016/j.desal.2010.07.004

Liu Z, Wu W, Shi P, Guo J, Cheng J (2015) Characterization of dissolved organic matter in landfill leachate during the combined treatment process of air stripping, Fenton, SBR and coagulation. Waste Manag 41:111–118. https://doi.org/10.1016/j.wasman.2015.03.044

Liu Y, Ying D, Sanguansri L, Cai Y, Le X (2018a) Adsorption of catechin onto cellulose and its mechanism study: kinetic models, characterization and molecular simulation. Food Res Int 112:225–232. https://doi.org/10.1016/j.foodres.2018.06.044

Liu Z, Li X, Rao Z, Hu F (2018b) Treatment of landfill leachate biochemical effluent using the nano-$Fe_3O_4/Na_2S_2O_8$ system: oxidation performance, wastewater spectral analysis, and activator characterization. J Environ Manage 208:159–168. https://doi.org/10.1016/j.jenvman.2017.12.023

Luo K, Pang Y, Li X, Chen F, Liao X, Lei M, Song Y (2018) Landfill leachate treatment by coagulation/flocculation combined with microelectrolysis–Fenton processes. Environ Technol. https://doi.org/10.1080/09593330.2018.1432694

Maaloul N, Oulego P, Rendueles M, Ghorbal A, Díaz M (2017) Novel biosorbents from almond shells: characterization and adsorption properties modeling for Cu(II) ions from aqueous solutions. J Environ Chem Eng 5:2944–2954. https://doi.org/10.1016/j.jece.2017.05.037

Mohammad-Pajooh E, Turcios AE, Cuff G, Weichgrebe D, Rosenwinkel K, Vedenyapina MD, Sharifullina LR (2018) Removal of inert COD and trace metals from stabilized landfill leachate by granular activated carbon (GAC) adsorption. J Environ Manage 228:189–196. https://doi.org/10.1016/j.jenvman.2018.09.020

Noh SJ, Schwarz AJ (1989) Estimation of the point of zero charge of simple oxides by mass titration. J Colloid Interface Sci 130:157–164

Oloibiri V, Ufomba I, Chys M, Audenaert WTM, Demeestere K, Van Hulle SWH (2015) A comparative study on the efficiency of ozonation and coagulation-flocculation as pretreatment to activated carbon adsorption of biologically stabilized landfill leachate. Waste Manag 43:335–342. https://doi.org/10.1016/j.wasman.2015.06.014

Omorogie MO, Babalola JO, Song W, Ru J, Unuabonah EI (2016) Efficient chromium abstraction from aqueous solution using a low-cost biosorbent: *Nauclea diderrichii* seed biomass waste. J Saudi Chem Soc 20:49–57. https://doi.org/10.1016/j.jscs.2012.09.017

Racar M, Dolar D, Špehar A, Kraš A, Košutić K (2017) Optimization of coagulation with ferric chloride as a pretreatment for fouling reduction during nanofiltration of rendering plant secondary effluent. Chemosphere 181:485–491. https://doi.org/10.1016/j.chemosphere.2017.04.108

Reynier N, Coudert L, Blais J, Mercier G, Besner S (2015) Treatment of contaminated soil leachate by precipitation, adsorption

and ion exchange. J Environ Chem Eng 3:977–985. https://doi.org/10.1016/j.jece.2015.03.002

Robinson T (2017) Removal of toxic metals during biological treatment of landfill leachates. Waste Manag 63:299–309. https://doi.org/10.1016/j.wasman.2016.12.032

Sruthi T, Gandhimathi R, Ramesh ST, Nidheesh PV (2018) Stabilized landfill leachate treatment using heterogeneous Fenton and electro-Fenton processes. Chemosphere 210:38–43. https://doi.org/10.1016/j.chemosphere.2018.06.172

Trabelsi I, Dhifallah T, Snoussi M, Benyahmed A, Fumio M, Saidi N, Jedidi N (2011) Cascade bioreactor with submerged biofilm for aerobic treatment of Tunisian landfill leachate. Bioresour Technol 102:7700–7706. https://doi.org/10.1016/j.biortech.2011.05.069

van Turnhout AG, Brandstätter C, Kleerebezem R, Fellner J, Heimovaara TJ (2018) Theoretical analysis of municipal solid waste treatment by leachate recirculation under anaerobic and aerobic conditions. Waste Manag 71:246–254. https://doi.org/10.1016/j.wasman.2017.09.034

Wang Z, Gao M, Li X, Ning J, Zhou Z, Li G (2019) Efficient adsorption of methylene blue from aqueous solution by graphene oxide modified persimmon tannins. Mater Sci Eng C 108:110196. https://doi.org/10.1016/j.msec.2019.110196

Wen X, Du C, Zeng G, Huang D, Zhang J, Yin L, Tan S, Huang L, Chen H, Yu G, Hu X, Lai C, Xu P, Wan J (2018) A novel biosorbent prepared by immobilized *Bacillus licheniformis* for lead removal from wastewater. Chemosphere 200:173–179. https://doi.org/10.1016/j.chemosphere.2018.02.078

Wu X, Lu C, Zhou Z, Xiong R, Zhang X (2014) Green synthesis and formation mechanism of cellulose nanocrystal-supported gold nanoparticles with enhanced catalytic performance. Environ Sci Nano 1:71–79. https://doi.org/10.1039/c3en00066d

Youcai Z (2018) Leachate generation and characteristics (Chap. 1). In: Pollution control technology for leachate from municipal solid waste. Elsevier BV, Oxford, pp 1–30

Zamri MFMA, Kamaruddin MA, Yusoff MS, Aziz HA, Foo KY (2017) Semi-aerobic stabilized landfill leachate treatment by ion exchange resin: isotherm and kinetic study. Appl Water Sci 7:581–590. https://doi.org/10.1007/s13201-015-0266-2

Zarghami Z, Akbari A, Mohammad A, Ali M (2016) Design of a new integrated chitosan-PAMAM dendrimer biosorbent for heavy metals removing and study of its adsorption kinetics and thermodynamics. Bioresour Technol 205:230–238. https://doi.org/10.1016/j.biortech.2016.01.052

Zazouli MA, Yousefi Z (2008) Removal of heavy metals from solid wastes leachates coagulation-flocculation process. J Appl Sci 8:2141–2147. https://doi.org/10.3923/jas.2008.2142.2147